DYNAMIC STRESS INTENSITY FACTOR FOR UNSTEADY RAPID CRACK PROPAGATION

K. ARAKAWA, T. MADA and K. TAKAHASHI

Research Institute for Applied Mechanics, Kyushu University, Kasuga 816-8580, Fukuoka, Japan

ABSTRACT

Dynamic crack propagation in PMMA was studied using the method of caustics in combination with a Cranz-Schardin type high-speed camera. Four different types of specimen geometries were employed to achieve the crack acceleration, deceleration and re-acceleration process in one fracture event. Dynamic stress intensity factor K_{ID} and crack velocity $\dot{a}$ were evaluated in the course of crack propagation to obtain the relationship between K_{ID} and $\dot{a}$. The effect of crack acceleration and deceleration on the K_{ID}-$\dot{a}$ relations was examined.

KEY WORDS

Dynamic crack propagation, stress intensity factor, crack velocity, crack acceleration, caustic method, high-speed photography, PMMA

INTRODUCTION

Dynamic crack propagation in brittle materials has been investigated using many experimental techniques. Optical methods such as photoelasticity [1-4] and the method of caustics [5-9] have been widely employed for evaluating the state of dynamic stress field around a propagating crack tip, i.e. dynamic stress intensity factor K_{ID}. Crack velocity $\dot{a}$ was also estimated in crack propagation to correlate with K_{ID}. Many experimental studies have been made on the relation between K_{ID} and $\dot{a}$, however, different experiments derived significantly different types of K_{ID}-$\dot{a}$ relationships. Much discussion has taken place on the applicability of the methods employed for K_{ID} evaluation, the definition of the crack tip stresses, the influence of specimen geometries and loading conditions and so forth. In the case of brittle fracture, $\dot{a}$ generally changes with time, resulting in crack acceleration or deceleration according to the stress distribution in the specimen. The crack acceleration is an important parameter to understand the behavior of dynamic crack propagation, however, quantitative discussion on the effect of the crack acceleration and deceleration on K_{ID} has been limited.

The purpose of the present work was to study this problem in more detail using the method of caustics in combination with a Cranz-Schardin type high-speed camera[10,11]. Four different types of specimen geometries were employed so that cracks could undergo acceleration, deceleration and re-acceleration stages in one fracture process. Dynamic stress intensity factor K_{ID} and crack velocity $\dot{a}$ were evaluated in the course of crack propagation. The K_{ID}-$\dot{a}$ relations were determined for the stages of acceleration, deceleration and/or re-acceleration. Attention was focussed particularly on the effect of the crack acceleration and deceleration on the K_{ID}-$\dot{a}$ relations.

EXPERIMENTAL PROCEDURE

Specimen geometries used in this experiment are illustrated in Fig. 1, where (a) represents a single-edge-notched (SEN) specimen, (b) a uniaxially pin-loaded specimen, (c) a biaxially pin-loaded specimen and (d) a SEN with two circular holes specimen. These four types of specimens were selected to obtain the different behaviors of dynamic crack propagation. The specimens were fabricated from a 5mm-thick sheet of PMMA (Acrylite S-001). A sharp precrack was generated by momentum-controlled chisel-impact into a pre-machined saw-cut on the specimen edge.

All specimens were tested under a displacement controlled condition using a tensile testing machine. Tests were performed at room temperature and at a constant crosshead speed of 1mm/min. The dynamic crack propagation was photographed using a Cranz-Schardin type high-speed camera with 30 sparks and a maximum frequency of 1.42×10^6 frames/sec [10,11]. This camera permitted a simultaneous record of two images with different focal distances. One focal distance was selected for specimen-focussed images and the other for caustic images.

EVALUATION OF K_{ID} AND CRACK VELOCITY $\dot{a}$

Figure 2 shows examples of high-speed photographs taken with a SEN specimen, where series (a) represents the specimen-focussed images and (b) the corresponding caustic patterns. As seen, size of the caustic changed with growing crack length. The stress intensity factor K_{ID} was determined from the following equation:

$$K_{ID} = (2\sqrt{2\pi}/3z_0 dc\eta^{3/2})(\phi/3.17)^{5/2} \qquad (1)$$

where ϕ is the caustic diameter at a crack tip, z_0 is the distance between the specimen and the image plane, d is the specimen thickness and η is a convergency factor for incident light rays [9].

The values of K_{ID} and crack length a obtained for the four specimens are shown in Figs. 3-6 as a function of time t. The K_{ID} variations for the specimens were different. In the SEN specimen under uniform tensile loading, K_{ID} increased in the initial stage of crack propagation and gradually approached a constant value. The uniaxially pin-loaded specimen exhibited K_{ID} increasing and decreasing behavior. In both the biaxially pin-loaded and SEN (Holes) specimens, there existed three stages of recognizable K_{ID} increasing, decreasing and re-increasing regions.

To minimize data scattering in the evaluation of fracture parameters, a data-fitting procedure which was proposed in a previous work [9] was employed; obtained values of K_{ID} and a were expressed as ninth order polynomial of t based on the least-squares method so that they

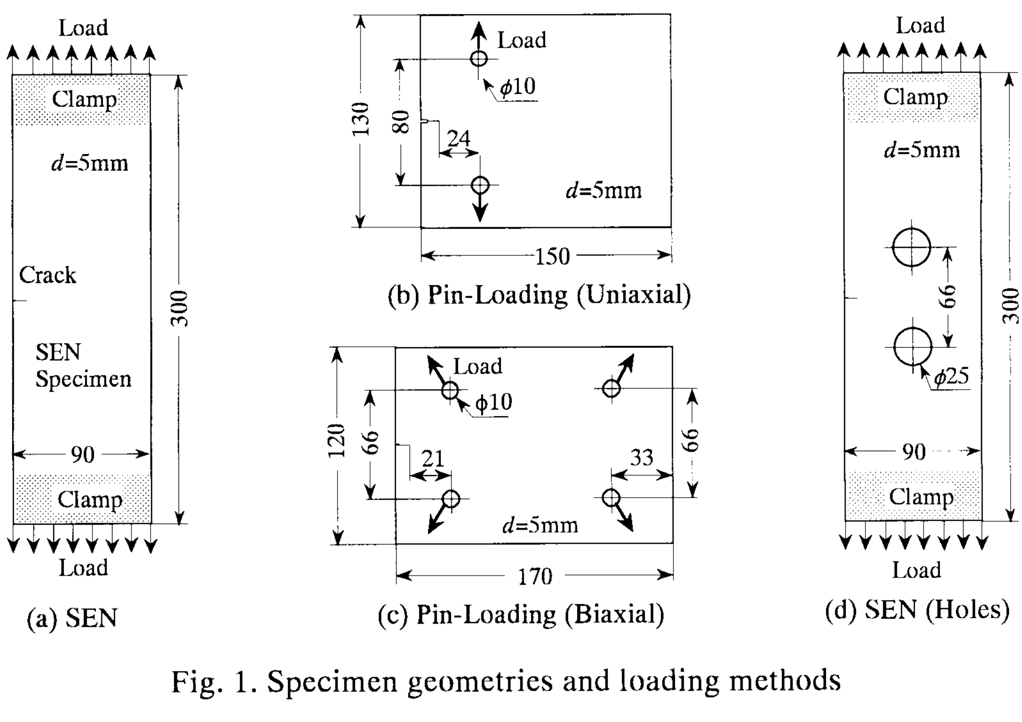

Fig. 1. Specimen geometries and loading methods

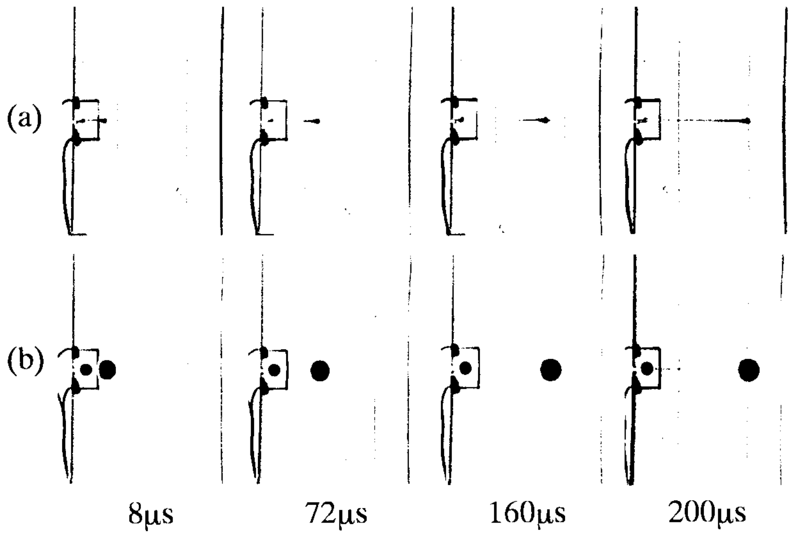

Fig. 2. Example of dynamic crack propagation in a SEN specimen.
(a) specimen-focussed images, (b) caustic patterns

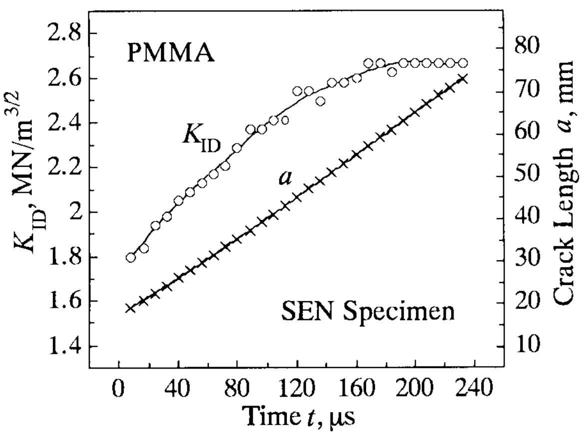

Fig. 3. Time variations of K_{ID} and crack length a for a SEN specimen

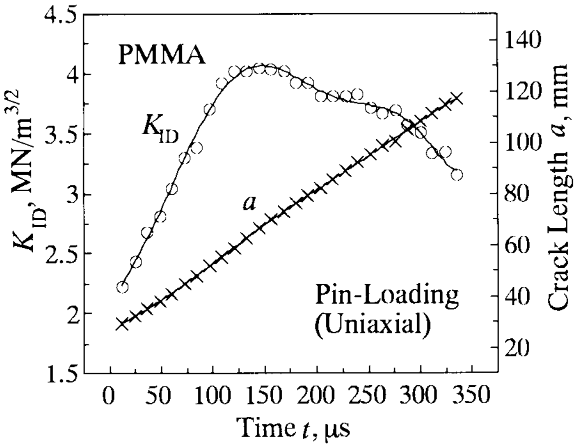

Fig. 4. Time variations of K_{ID} and crack length a for a uniaxially pin-loaded specimen

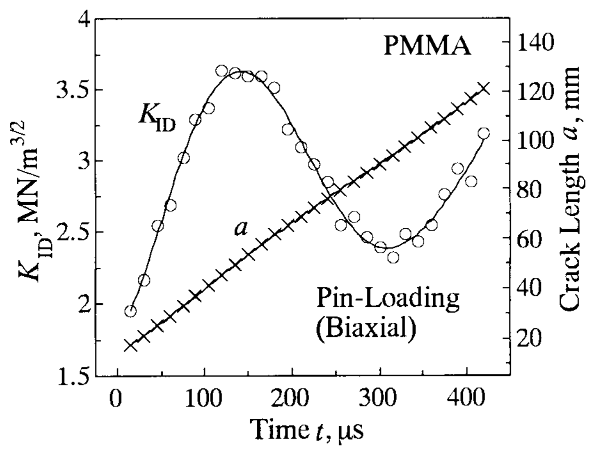

Fig. 5. Time variations of K_{ID} and crack length a for a biaxially pin-loaded specimen

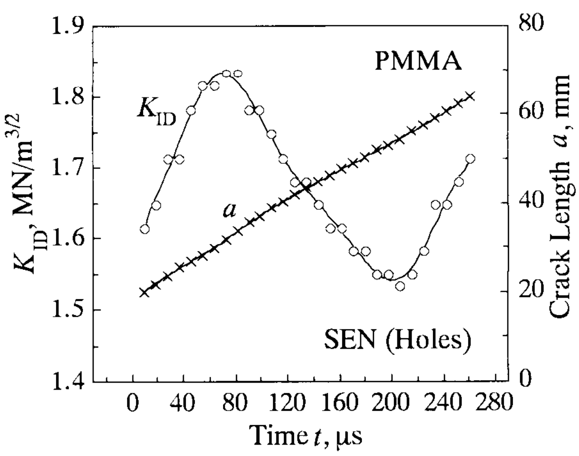

Fig. 6. Time variations of K_{ID} and crack length a for a SEN with holes specimen

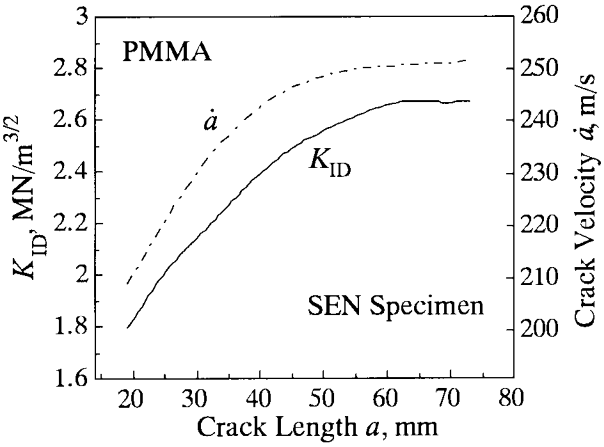

Fig. 7. K_{ID} and crack velocity $\dot{a}$ for a SEN specimen

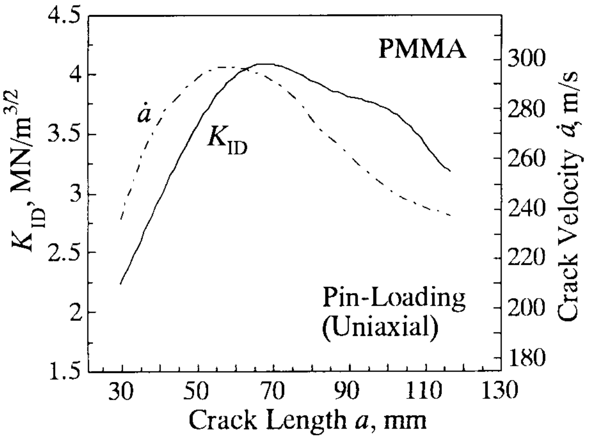

Fig. 8. K_{ID} and crack velocity $\dot{a}$ for a uniaxially pin-loaded specimen

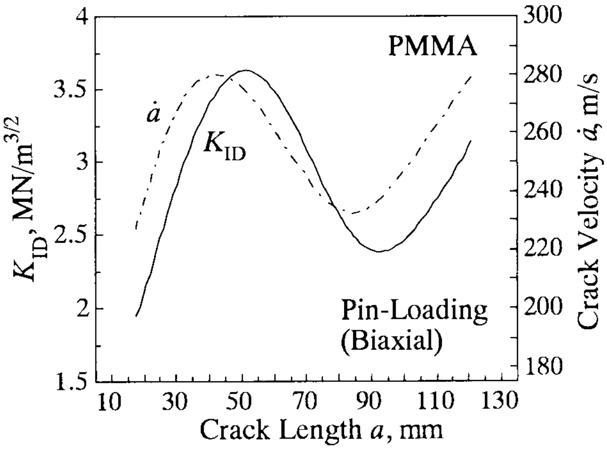

Fig. 9. K_{ID} and crack velocity $\dot{a}$ for a biaxially pin-loaded specimen

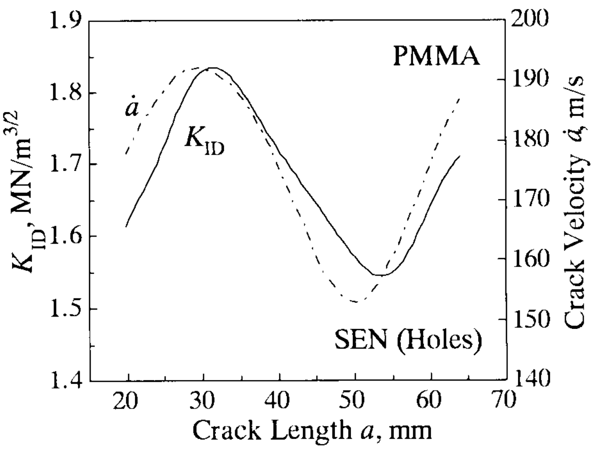

Fig. 10. K_{ID} and crack velocity $\dot{a}$ for a SEN with holes specimen

closely fitted their observed values (see Figs. 3-6). Crack velocity $\dot{a}$ was determined from the first time derivatives of the fitted curve $a(t)$. If $\dot{a}$ was determined simply from the first time derivative of increment Δa which was obtained from successive pictures taken on a film, large scatter in $\dot{a}$ was inevitably caused primarily by errors arising from visual identification of the crack tip position on film. Thus, the data-fitting procedure employed enabled us to determine crack velocity accurately.

RELATIONSHIPS BETWEEN K_{ID} AND $\dot{a}$

Figures 7-10 show values of K_{ID} and $\dot{a}$ as a function of crack length a. There are several interesting points in their relations. First, the change in $\dot{a}$ was qualitatively in accord with the one in K_{ID}. Second, $\dot{a}$ rose earlier than K_{ID} associated with a. Finally, K_{ID} for a constant $\dot{a}$ was larger when the crack was decelerated than when it was accelerated (see Figs. 8-10). Similar results were also obtained by the authors for epoxy and Homalite-100 specimens [12-15].

To study the effect of the crack acceleration and deceleration, the values of K_{ID} were expressed as a function of $\dot{a}$. Figures 11-14 show $K_{ID}(\dot{a})$ curves, where arrows indicate the direction of progress of the fracture. The open circles represent the acceleration-free points ($\ddot{a}$=0) obtained from the maximum and minimum velocity positions. There are several interesting points in the K_{ID}-$\dot{a}$ relations. First, $K_{ID}(\dot{a})$ for the SEN specimen only exhibited the increasing process so that it gradually approached a constant value. Second, distinct crack

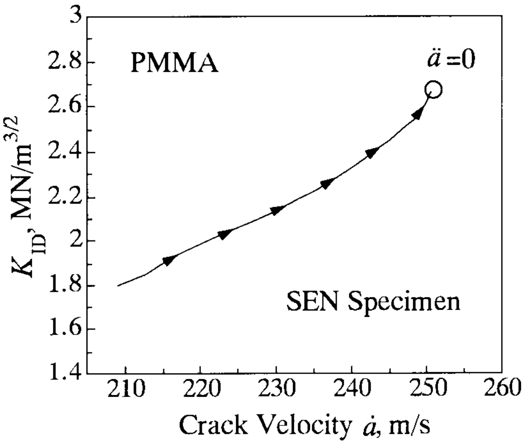

Fig. 11. K_{ID}-$\dot{a}$ relation for a SEN specimen under unifrom tensile loading

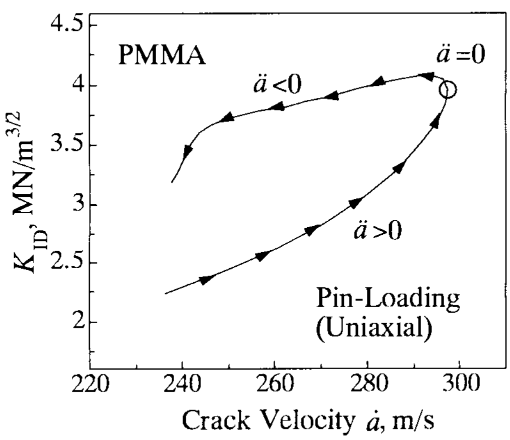

Fig. 12. K_{ID}-$\dot{a}$ relation for a uniaxially pin-loaded specimen

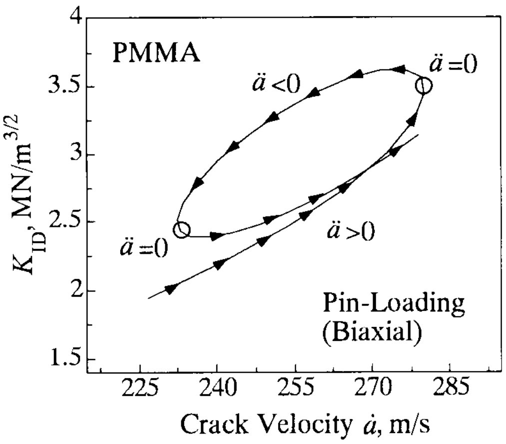

Fig. 13. K_{ID}-$\dot{a}$ relation for a biaxially pin-loaded specimen

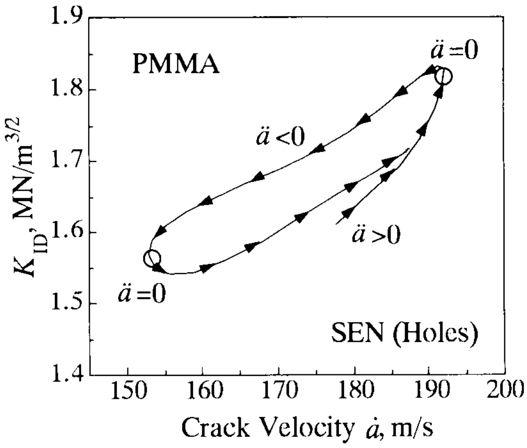

Fig. 14. K_{ID}-$\dot{a}$ relation for a SEN with holes specimen

acceleration ($\ddot{a}>0$) and deceleration ($\ddot{a}<0$) can be seen in the uniaxially pin-loaded specimen. Finally, in both the biaxially pin-loaded and SEN (Holes) specimens, three stages of distinct crack acceleration ($\ddot{a}>0$), deceleration ($\ddot{a}<0$) and re-acceleration ($\ddot{a}>0$) can be seen in one fracture process. Although $K_{ID}(\dot{a})$ is shown to increase with $\dot{a}$, it should be noted that their relation was not unique. For a constant $\dot{a}$, the decelerating crack had a larger value of K_{ID} than the accelerating or re-accelerating one. Such was also the case with other specimens tested.

The authors have suggested that K_{ID} was expressed as two parametric functions of $\dot{a}$ and $\ddot{a}$, i.e. $K_{ID}(\dot{a}, \ddot{a})$, and that $K_{ID}(\dot{a}, \ddot{a}\text{=constant})$ was uniquely related to $\dot{a}$ [9,12,13]. This was examined using the obtained results. Figure 15 shows the $K_{ID}(\dot{a})$ curves determined for the four specimens. The dotted curve of $K_{ID}(\dot{a}, \ddot{a}=0)$ connecting the acceleration free points can separate the acceleration ($\ddot{a}>0$) and deceleration ($\ddot{a}<0$) area in the K_{ID}-$\dot{a}$ diagram. As seen, $K_{ID}(\dot{a})$ for a constant $\dot{a}$ had a larger value when the crack was decelerated than when it was accelerated, i.e. $K_{ID}(\dot{a}, \ddot{a}<0) > K_{ID}(\dot{a}, \ddot{a}>0)$. It should be noted that $K_{ID}(\dot{a}, \ddot{a}=0)$ can be uniquely related to $\dot{a}$ as suggested in previous studies [9,13]. Hence, this clearly appears to indicate that $K_{ID}(\dot{a}, \ddot{a}=0)$ can be the material property, while the time variations of K_{ID} and $\dot{a}$ were strongly influenced by specimen geometries and loading methods as shown in Figs 7-10.

CONCLUSIONS

Dynamic crack propagation in PMMA was studied using the method of caustics and a Cranz-Schardin high-speed camera. Four different types of specimen geometries were employed to achieve the crack acceleration, deceleration and re-acceleration process in one fracture event. Dynamic stress intensity factor K_{ID} and crack velocity $\dot{a}$ were evaluated, and the following findings were obtained:

(1) The variations of K_{ID} and $\dot{a}$ were strongly influenced by the specimen geometries and loading methods.
(2) $\dot{a}$ change was qualitatively in accord with the one in K_{ID}.
(3) K_{ID} for a constant $\dot{a}$ was larger when the crack was decelerated than when it was accelerated or re-accelerated.
(4) K_{ID} for acceleration-free can be uniquely related to $\dot{a}$.

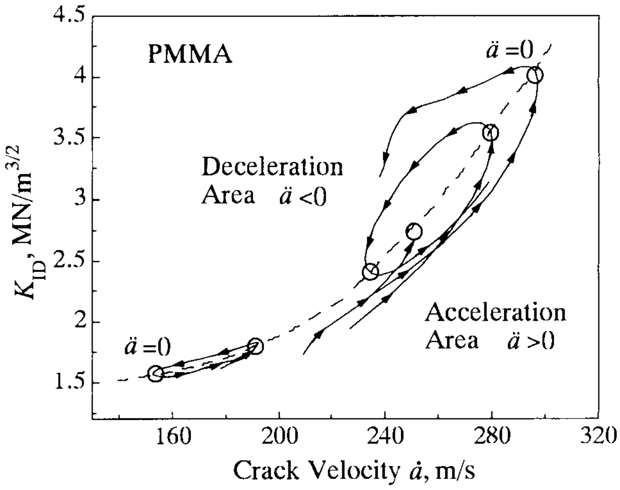

Fig. 15. K_{ID}-$\dot{a}$ curves for the four different types of PMMA specimens

REFERENCES

1. J.W. Dally, W.L. Fourney and G.R. Irwin (1985) "On the uniqueness of the stress intensity factor - crack velocity relationship", *Int. J. Fracture*, **27**, 159-168.
2. A.S. Kobayashi, M. Ramulu, M.S. Dadkhah, K.-H. Yang and B.S.J. Kang (1986) "Dynamicfracture toughness" *Int. J. Fracture*, **30**, 275-285.
3. A. Shukla and H. Nigam (1986) "A note on the stress intensity factor and crack velocity relationship for Homalite 100" *Engng Fracture Mech.,* **25**, 91-102.
4. J.W. Dally, R.K. Agarwal and R.J. Sanford (1990) "A study of hysteresis in the K_{ID}-$\dot{a}$ relation" *Exp. Mech.,* **30**, 177-183.
5. J.F. Kalthoff (1983) "On some current problems in experimental fracture dynamics" In W.G.Knauss (ed.), *Workshop on Dynamic Fracture,* California Institute of Technology, Pasadena,11-35.
6. W.G. Knauss and K. Ravi-Chandar (1985) "Some basic problems in stress wave dominated fracture" *Int. J. Fracture*, **27**, 127-143.
7. T. Nishioka, T. Murakami, H. Uchiyama, K. Sakakura and H. Kittaka (1991) "Specimen size effects on dynamic crack propagation and arrest in DCB specimens" *Engng Fracture Mech.,* **39**, 757-767.
8. A.J. Rosakis (1993) "Two optical techniques sensitive to gradients of optical path difference: the method of caustics and the coherent gradient sensor (CGS)" In J.S. Epstein (ed.), *Experimental Techniques in Fracture*, VCH Publishers, 327-425.
9. K. Takahashi and K. Arakawa (1987) "Dependence of crack acceleration on the dynamic stress - intensity factor in polymers" *Exp. Mech.,* **27**, 195-200.
10. K. Arakawa and K. Takahashi (1991) "Branching of a fast crack in polymers" *Int. J. Fracture*, **48**, 245-259.
11. K. Takahashi and T. Mada (1993) "Dual-focus high-speed photography and its application to fracture and impact studies" In J.M. Dewey and R.G. Racca (eds.), *20th International Congress on High-Speed Photography and Photonics,* SPIE 1802, 901-909.
12. K. Arakawa and K. Takahashi (1991) "Relationships between fracture parameters and fracture surface roughness of brittle polymers" *Int. J. Fracture*, **48**, 103-114.
13. K. Arakawa, D. Nagoh and K. Takahashi (1997) "Crack velocity and acceleration effects on the dynamic stress intensity factor in polymers" *Int. J. Fracture*, **83**, 305-313.
14. K. Takahashi, M. Kido and K. Arakawa (1998) "Fracture roughness evolution during mode I dynamic crack propagation in brittle materials" *Int. J. Fracture*, **90**, 119-131.
15. K. Arakawa, D. Nagoh and K. Takahashi (1999) "Dynamic Crack propagation and unloading behavior of brittle polymers" *Int. J. Fracture*, **96**, 345-358.